Equivalence Between Short-Time Biphasic and Incompressible Elastic Material Responses

Gerard A. Ateshian

Departments of Mechanical Engineering and
Biomedical Engineering,
Columbia University,
New York, NY 10027

Benjamin J. Ellis

Jeffrey A. Weiss

Department of Bioengineering and Scientific
Computing and Imaging Institute,
University of Utah,
Salt Lake City, UT

Porous-permeable tissues have often been modeled using porous media theories such as the biphasic theory. This study examines the equivalence of the short-time biphasic and incompressible elastic responses for arbitrary deformations and constitutive relations from first principles. This equivalence is illustrated in problems of unconfined compression of a disk, and of articular contact under finite deformation, using two different constitutive relations for the solid matrix of cartilage, one of which accounts for the large disparity observed between the tensile and compressive moduli in this tissue. Demonstrating this equivalence under general conditions provides a rationale for using available finite element codes for incompressible elastic materials as a practical substitute for biphasic analyses, so long as only the short-time biphasic response is sought. In practice, an incompressible elastic analysis is representative of a biphasic analysis over the short-term response $\delta t \ll \Delta^2 / \sqrt[4]{\|\mathbf{C}\|} \sqrt[4]{\|\mathbf{K}\|}$, where Δ is a characteristic dimension, $\mathbf{C}$ is the elasticity tensor, and $\mathbf{K}$ is the hydraulic permeability tensor of the solid matrix. Certain notes of caution are provided with regard to implementation issues, particularly when finite element formulations of incompressible elasticity employ an uncoupled strain energy function consisting of additive deviatoric and volumetric components. [DOI: 10.1115/1.2720918]

Introduction

Hydrated soft tissues have been successfully modeled using porous media theories, which account for deformation of the solid matrix and flow of interstitial fluid. For articular cartilage, the biphasic theory of Mow et al. [1], which models the tissue as a mixture of a solid phase and a fluid phase, and its subsequent refinements which account for tension-compression nonlinearity of the fibrillar solid matrix [2–4], has demonstrated very good agreement with experimental results. This theory captures the flow-dependent viscoelasticity under a variety of loading conditions. The transient viscoelastic response depends on the material properties and permeability of the solid matrix and the characteristic dimensions of the tissue. For cartilage, the transient response lasts for hundreds or thousands of seconds.

Theoretical studies have shown that the instantaneous response of a biphasic material to a step load is equivalent to that of an incompressible elastic solid. This equivalence, which stems from the intrinsic incompressibility of the solid and fluid phases [5], has been established for small strain and isotropic material symmetry, in specific problems such as confined and unconfined compression [1,4,6,7], indentation [8], and contact with a spherical indenter [9].

The objective of this study is to establish the equivalence of the instantaneous biphasic and incompressible elastic responses for arbitrary deformations and constitutive relations from first principles, and to provide practical guidelines for the validity of this equivalence over the short-term biphasic response. Furthermore, since the constitutive relation of the solid matrix of a biphasic material is generally formulated for compressible materials, to account for the loss of tissue volume with fluid efflux, specific guidelines are provided regarding the equivalence of finite deformation anisotropic constitutive relations in the biphasic and incompressible elastic formulations. This equivalence is illustrated in a problem of articular contact under finite deformation, using two different constitutive relations for the solid matrix of cartilage, one of which accounts for the large disparity observed between the tensile and compressive moduli in this tissue [10–13]. Demonstrating this equivalence under general conditions provides a rationale for using available finite element codes for incompressible elastic materials as a practical substitute for biphasic contact analyses, as long as only the short-time biphasic response is sought. It also provides insight into the interpretation of earlier incompressible and nearly-incompressible elastic analyses of articular cartilage [14–17].

Methods

Biphasic Material. The Cauchy stress $\mathbf{T}$ in a biphasic material is the sum of the interstitial fluid pressure, p, and the elastic stress in the solid matrix, $\mathbf{T}^e$,

$$\mathbf{T} = -p\mathbf{I} + \mathbf{T}^e \tag{1}$$

The frictional drag on the solid matrix due to the flow of interstitial fluid is denoted by $\boldsymbol{\pi}$. Conservation of linear momentum for the biphasic mixture and the interstitial fluid yields, respectively,

$$\operatorname{div} \mathbf{T} = \mathbf{0} \tag{2}$$

$$\varphi^w \operatorname{grad} p + \boldsymbol{\pi} = \mathbf{0} \tag{3}$$

where φ^w is the solid matrix porosity. Conservation of mass for the mixture requires that

$$\operatorname{div}(\mathbf{v} + \mathbf{w}) = 0 \tag{4}$$

where $\mathbf{v} = D\mathbf{u}/Dt$ is the solid matrix velocity, $\mathbf{u}$ is the solid displacement, and $\mathbf{w}$ is the flux of the interstitial fluid relative to the solid. It is necessary to specify constitutive models for $\mathbf{T}^e$ and $\boldsymbol{\pi}$, which may be a function of solid matrix strain and relative fluid flux, respectively. The boundary conditions for a biphasic material are given by

$$\mathbf{Tn} = \mathbf{t}^* \text{ or } \mathbf{u} = \mathbf{u}^* \tag{5}$$

$$p = p^* \quad \text{or} \quad \mathbf{w} \cdot \mathbf{n} = w_n^* \tag{6}$$

where $\mathbf{t}^*$ is a prescribed traction on a boundary of unit outward normal $\mathbf{n}$, $\mathbf{u}^*$ is a prescribed displacement, p^* is a prescribed fluid pressure, and w_n^* is a prescribed fluid flux normal to the boundary.

Incompressible Elastic Material. For an incompressible elastic solid the Cauchy stress is given by

$$\mathbf{T} = -\bar{p}\mathbf{I} + \bar{\mathbf{T}}^e \tag{7}$$

In this case $\bar{p}$ represents a pressure resulting from the incompressibility constraint; $\bar{\mathbf{T}}^e$ represents the remaining stress in the solid. The conservation of linear momentum and mass are given by

$$\text{div } \mathbf{T} = \mathbf{0} \tag{8}$$

$$\text{div } \mathbf{v} = \frac{1}{J}\frac{DJ}{Dt} = 0 \tag{9}$$

where $J = \det \mathbf{F}$ and $\mathbf{F} = \mathbf{I} + \text{Grad } \mathbf{u}$ is the deformation gradient. Equation (9) and its corresponding initial condition ($\mathbf{u} = \mathbf{0}$, $J = 1$ at $t = 0$) are equivalent to stating that $J = 1$ for all t. The boundary conditions are

$$\mathbf{Tn} = \mathbf{t}^* \quad \text{or} \quad \mathbf{u} = \mathbf{u}^* \tag{10}$$

Note that there are no boundary conditions on $\bar{p}$.

Equivalence. Upon sudden loading of a biphasic material, at time $t = 0^+$, the interstitial fluid has not had time to leave the tissue (solid matrix pores change shape but not volume), except at permeable boundaries where the fluid can escape. This does not imply that the fluid flux is zero, but rather div $\mathbf{w}|_{t=0^+} = 0$ everywhere, except at permeable boundaries. Now the conservation of mass for a biphasic material, Eq. (4), reduces to that of an elastic incompressible material, Eq. (9). At this stage it is noted that the constitutive relations for $\mathbf{T}^e$ and $\bar{\mathbf{T}}^e$ should be constructed to be identical when $J = 1$,

$$\mathbf{T}^e|_{J=1} = \bar{\mathbf{T}}^e \tag{11}$$

Given this constraint, since Eqs. (7)–(10) have the exact same form as Eqs. (1), (2), (4), and (5) at $t = 0^+$, the solid displacement $\mathbf{u}$ and stress $\mathbf{T}$ are *exactly the same* for the instantaneous biphasic and incompressible elastic responses, and $\bar{p} = p$ everywhere *except at permeable boundaries where $p = p^*$ is prescribed*. In fact, Eq. (3) can be used to determine the frictional drag $\boldsymbol{\pi}$ everywhere other than on permeable boundaries.

Thus the response of a biphasic material at $t = 0^+$ is equivalent to that of an incompressible elastic material, with identical $\mathbf{u}$ and $\mathbf{T}$ throughout the material, and $p = \bar{p}$ everywhere except in an infinitely thin boundary layer at permeable boundaries. This result agrees with observations made in the theoretical solutions of specific biphasic problems [1,4,6–9].

Examples of Constitutive Relations

Frictional Drag. The frictional or diffusive drag is commonly related to the relative fluid flux through

$$\boldsymbol{\pi} = \varphi^w \mathbf{K}^{-1} \mathbf{w} \tag{12}$$

where $\mathbf{K}$ is the hydraulic permeability tensor [18,19]. Substituting this relation into Eq. (3) yields Darcy's law, $\mathbf{w} = -\mathbf{K} \text{ grad } p$. In the case of isotropic permeability we have $\mathbf{K} = k\mathbf{I}$, where k may be given, for example, by the formulation of Holmes and Mow [20],

$$k = k_0 \left[\frac{(1 - \varphi_0^w)\varphi^w}{(1 - \varphi^w)\varphi_0^w} \right]^\alpha e^{M(J^2 - 1)/2} \tag{13}$$

Here, k is the hydraulic permeability of the matrix, k_0 is its value at $J = 1$, and φ_0^w is the matrix porosity at $J = 1$, with

$$\varphi^w = 1 - \frac{1 - \varphi_0^w}{J} \tag{14}$$

as can be derived from the conservation of mass. The unitless material coefficients M and α control the nonlinear dependence of k on matrix dilatation. Setting $\alpha = 0$ yields the more traditional form used by Lai et al. [21], while letting $M = 0$ yields the form advocated by Gu et al. [22].

Constitutive Models for the Solid Matrix. In principle, any well-posed constitutive model may be used for the solid matrix of a biphasic material. If the strain energy density is given by $W(\mathbf{C})$, where $\mathbf{C} = \mathbf{F}^T\mathbf{F}$ is the right Cauchy-Green strain tensor, then the stress and spatial elasticity tensors are given by [23]

$$\mathbf{T}^e = 2J^{-1}\mathbf{F}\frac{\partial W}{\partial \mathbf{C}}\mathbf{F}^T \tag{15}$$

$$\overset{4}{\mathbf{C}} = 4J^{-1}(\mathbf{F} \underline{\otimes} \mathbf{F}) : \frac{\partial^2 W}{\partial \mathbf{C}^2} : (\mathbf{F}^T \underline{\otimes} \mathbf{F}^T) \tag{16}$$

The definitions of the tensor double dot product : and dyadic product $\otimes$ are given in the Appendix. For example, a compressible neo-Hookean material is given by [23]

$$W = \frac{\mu}{2}(I_1 - 3) - \mu \ln J + \frac{\lambda}{2}(\ln J)^2 \tag{17}$$

$$\mathbf{T}^e = J^{-1}[\mu(\mathbf{B} - \mathbf{I}) + \lambda(\ln J)\mathbf{I}] \tag{18}$$

$$\overset{4}{\mathbf{C}} = J^{-1}[\lambda \mathbf{I} \otimes \mathbf{I} + 2(\mu - \lambda \ln J)\mathbf{I}\bar{\underline{\otimes}}\mathbf{I}] \tag{19}$$

where $\mathbf{B} = \mathbf{F}\mathbf{F}^T$ is the left Cauchy-Green strain tensor, $I_1 = \text{tr } \mathbf{C} = \text{tr } \mathbf{B}$, and λ and μ are Lamé-type moduli. The definitions of the tensor dyadic products $\otimes$ and $\bar{\underline{\otimes}}$ are provided in the Appendix. It follows from Eq. (11) that the stress for the corresponding incompressible elastic solid is

$$\bar{\mathbf{T}}^e = \mathbf{T}^e|_{J=1} = \mu(\mathbf{B} - \mathbf{I}) \tag{20}$$

In many computational implementations of incompressible elasticity [24,25], the strain energy density is assumed to take an uncoupled form, consisting of additive deviatoric and volumetric components in the form

$$W(\mathbf{C}) = \tilde{W}(\tilde{\mathbf{C}}) + U(J) \tag{21}$$

where $\tilde{\mathbf{C}} = \tilde{\mathbf{F}}^T\tilde{\mathbf{F}}$ and $\tilde{\mathbf{F}} = J^{-1/3}\mathbf{F}$ is the deviatoric part of the deformation gradient. The assumption of an uncoupled strain energy is based more on mathematical and computational convenience rather than physical observation—all finite element implementations of nearly-incompressible elasticity require a separate interpolation of the pressure term to avoid element locking, and with the form specified by Eq. (21) the entire pressure arises from $U(J)$. It should be noted that this uncoupled form explicitly assumes that there is no term in the strain energy that depends on both $\tilde{\mathbf{C}}$ and J. Using the chain rule of differentiation, the stress and spatial elasticity tensors for the strain energy in Eq. (21) are

$$\mathbf{T}^e = \tilde{\mathbf{T}}^e - \frac{1}{3}(\tilde{\mathbf{T}}^e : \mathbf{I})\mathbf{I} + \frac{dU}{dJ}\mathbf{I} = \text{dev } \tilde{\mathbf{T}}^e + \frac{dU}{dJ}\mathbf{I} \tag{22}$$

$$\overset{4}{\mathbf{C}} = \frac{d}{dJ}\left(J\frac{dU}{dJ}\right)\mathbf{I}\otimes\mathbf{I} - 2\frac{dU}{dJ}\mathbf{I}\,\overline{\underline{\otimes}}\,\mathbf{I}$$
$$+ \frac{2}{3}\left[(\widetilde{\mathbf{T}}^e{:}\mathbf{I})\left(\mathbf{I}\,\overline{\underline{\otimes}}\,\mathbf{I} + \frac{1}{3}\mathbf{I}\otimes\mathbf{I}\right) - (\mathbf{I}\otimes\widetilde{\mathbf{T}}^e + \widetilde{\mathbf{T}}^e\otimes\mathbf{I})\right]$$
$$+ \overset{4}{\widetilde{\mathbf{C}}} - \frac{1}{3}\left[\mathbf{I}\otimes\mathbf{I}{:}\overset{4}{\widetilde{\mathbf{C}}} + \overset{4}{\widetilde{\mathbf{C}}}{:}\mathbf{I}\otimes\mathbf{I} - \frac{1}{3}(\mathbf{I}{:}\overset{4}{\widetilde{\mathbf{C}}}{:}\mathbf{I})\mathbf{I}\otimes\mathbf{I}\right] \tag{23}$$

where

$$\widetilde{\mathbf{T}}^e = 2J^{-1}\widetilde{\mathbf{F}}\frac{\partial\widetilde{W}}{\partial\widetilde{\mathbf{C}}}\widetilde{\mathbf{F}}^T \tag{24}$$

$$\overset{4}{\widetilde{\mathbf{C}}} = 4J^{-1}(\widetilde{\mathbf{F}}\,\underline{\otimes}\,\widetilde{\mathbf{F}}){:}\frac{\partial^2\widetilde{W}}{\partial\widetilde{\mathbf{C}}^2}{:}(\widetilde{\mathbf{F}}^T\,\underline{\otimes}\,\widetilde{\mathbf{F}}^T) \tag{25}$$

and the operator dev[·] extracts the deviatoric part of a second-order tensor with both legs in the spatial configuration

$$\mathrm{dev}[\cdot] = [\cdot] - \frac{1}{3}([\cdot]{:}\mathbf{I})\mathbf{I} \tag{26}$$

An example of an uncoupled strain energy density function is a modified compressible neo-Hookean solid of the form

$$W = \frac{1}{2}[\mu(\widetilde{I}_1 - 3) + \kappa(\ln J)^2] \tag{27}$$

where $\widetilde{I}_1 = \mathrm{tr}\,\widetilde{\mathbf{C}} = \mathrm{tr}\,\widetilde{\mathbf{B}} = J^{-2/3}I_1$, $\widetilde{\mathbf{B}} = J^{-2/3}\mathbf{B}$, and $\kappa = \lambda + 2\mu/3$ is the bulk modulus. In this expression it is noted that $\widetilde{W} = \mu(\widetilde{I}_1 - 3)/2$ and $U = \kappa(\ln J)^2/2$. The stress and spatial elasticity tensors for this material are given by

$$\mathbf{T}^e = J^{-1}\left[\kappa(\ln J)\mathbf{I} + \mu\left(\widetilde{\mathbf{B}} - \frac{1}{3}\widetilde{I}_1\mathbf{I}\right)\right] \tag{28}$$

$$\overset{4}{\mathbf{C}} = J^{-1}\left[2\left(\frac{\mu}{3}\widetilde{I}_1 - \kappa\ln J\right)\mathbf{I}\,\overline{\underline{\otimes}}\,\mathbf{I} + \left(\kappa + \frac{2\mu}{9}\widetilde{I}_1\right)\mathbf{I}\otimes\mathbf{I}\right.$$
$$\left. - \frac{2}{3}\mu(\mathbf{I}\otimes\widetilde{\mathbf{B}} + \widetilde{\mathbf{B}}\otimes\mathbf{I})\right] \tag{29}$$

In the limit of an incompressible elastic solid,

$$\bar{\mathbf{T}}^e = \left.\mathbf{T}^e\right|_{J=1} = \mu\left(\widetilde{\mathbf{B}} - \frac{1}{3}\widetilde{I}_1\mathbf{I}\right) \tag{30}$$

A practical advantage of this specific constitutive relation is that $\mathrm{tr}\,\bar{\mathbf{T}}^e = 0$, which implies that the pressure $\bar{p}$, which is equivalent to the fluid pressure in the instantaneous biphasic response, is simply given by the hydrostatic part of the total stress, $\bar{p} = -\mathrm{tr}\,\bar{\mathbf{T}}/3$.

Tension-Compression Nonlinearity. There are several related ways to incorporate tension-compression nonlinearity in a constitutive relation [3,26–30]. In this illustrative example we extend the approach of Quapp and Weiss [27] to the case of a tissue with three preferred and mutually orthogonal material directions. For articular cartilage these directions are defined as (1) parallel to the split line direction, (2) perpendicular to the split line direction, and (3) normal to the articular surface, and these directions are represented by the unit vectors $\mathbf{a}_a^0$ ($a=1-3$) in the reference configuration [4]. The constitutive relation for the strain energy is supplemented by terms which are only functions of the normal stretch $\lambda_a = (\mathbf{a}_a^0\cdot\mathbf{C}\mathbf{a}_a^0)^{1/2}$ along each of the three directions $\mathbf{a}_a^0$,

$$W = W_0 + \sum_{a=1}^{3}\Psi_a(\lambda_a) \tag{31}$$

It follows from Eqs. (15) and (16) that the stress and elasticity tensors are given by

$$\mathbf{T}^e = \mathbf{T}_0^e + J^{-1}\sum_{a=1}^{3}\lambda_a\frac{\partial\Psi_a}{\partial\lambda_a}\mathbf{A}_a \tag{32}$$

$$\overset{4}{\mathbf{C}} = \overset{4}{\mathbf{C}}_0 + J^{-1}\sum_{a=1}^{3}\lambda_a^3\frac{\partial}{\partial\lambda_a}\left(\frac{1}{\lambda_a}\frac{\partial\Psi}{\partial\lambda_a}\right)\mathbf{A}_a\otimes\mathbf{A}_a \tag{33}$$

where the dependence of $\mathbf{T}_0^e$ and $\overset{4}{\mathbf{C}}_0$ on W_0 is given in Eqs. (15) and (16). In these expressions the texture tensors $\mathbf{A}_a = \mathbf{a}_a\otimes\mathbf{a}_a$ can be evaluated from $\mathbf{a}_a = \mathbf{F}\mathbf{a}_a^0/\lambda_a$.

For example, motivated by our recent study [11], the function Ψ_a may be given by

$$\Psi_a = \begin{cases} \xi_a(\lambda_a - 1)^{\beta_a} & \lambda_a > 1 \\ 0 & \lambda_a \leqslant 1 \end{cases} \qquad \xi_a \geqslant 0 \ \beta_a \geqslant 2 \tag{34}$$

The strain energy component Ψ_a makes a contribution only when the stretch is tensile along the corresponding direction. The material coefficients ξ_a and β_a regulate the tensile response along the three preferred material directions. For the special case $\beta_a = 2$ the modulus exhibits a jump at the strain origin as assumed in some of our earlier studies [4], whereas $\beta_a > 2$ produces a smooth transition more akin to recent experimental observations [11,31].

Any suitable function W_0 may be selected, as given for example in Eq. (17). However, if an uncoupled representation of the strain energy density is desired, as given in Eq. (27) for example, it is not possible to uncouple the constitutive relation for $\Psi_a(\lambda_a)$ into deviatoric and dilatational parts, because $\lambda_a = J^{1/3}\widetilde{\lambda}_a$, where $\widetilde{\lambda}_a = (\mathbf{a}_a^0\cdot\widetilde{\mathbf{C}}\mathbf{a}_a^0)^{1/2}$. Thus Ψ_a cannot be written as the sum of a term depending only on $\widetilde{\lambda}_a$ and another depending only on J. In general, it may not be acceptable in the biphasic implementation to substitute $\Psi_a(\lambda_a)$ with a function $\widetilde{\Psi}_a(\widetilde{\lambda}_a)$, since $\widetilde{\lambda}_a$ and λ_a have different physical meanings for deformations that are not isochoric. As an example, it is possible for one to be less than unity while the other is greater for nonisochoric deformations, invalidating the conditional clause of tension-compression nonlinearity as illustrated in Eq. (34). The only exception is in the instantaneous biphasic response, when $J=1$, which leads to $\lambda_a = \widetilde{\lambda}_a$. Then, based on Eqs. (21)–(23), the strain energy, stress, and elasticity tensors would be given by

$$W = W_0 + \sum_{a=1}^{3}\widetilde{\Psi}_a(\widetilde{\lambda}_a) \tag{35}$$

$$\mathbf{T}^e = \mathbf{T}_0^e + J^{-1}\sum_{a=1}^{3}\widetilde{\lambda}_a\frac{\partial\widetilde{\Psi}_a}{\partial\widetilde{\lambda}_a}\left(\mathbf{A}_a - \frac{1}{3}\mathbf{I}\right) \tag{36}$$

$$\overset{4}{\mathbf{C}} = \overset{4}{\mathbf{C}}_0 + J^{-1}\sum_{a=1}^{3}\widetilde{\lambda}_a\frac{\partial\widetilde{\Psi}_a}{\partial\widetilde{\lambda}_a}\left[\frac{2}{3}\mathbf{I}\,\overline{\underline{\otimes}}\,\mathbf{I} - \frac{1}{3}\left(\mathbf{I}\otimes\mathbf{A}_a + \mathbf{A}_a\otimes\mathbf{I} - \frac{1}{3}\mathbf{I}\otimes\mathbf{I}\right)\right.$$
$$\left. - \mathbf{A}_a\otimes\mathbf{A}_a\right] + \widetilde{\lambda}_a^2\frac{\partial^2\widetilde{\Psi}_a}{\partial\widetilde{\lambda}_a^2}$$
$$\times\left[\mathbf{A}_a\otimes\mathbf{A}_a - \frac{1}{3}\left(\mathbf{I}\otimes\mathbf{A}_a + \mathbf{A}_a\otimes\mathbf{I} - \frac{1}{3}\mathbf{I}\otimes\mathbf{I}\right)\right] \tag{37}$$

Comparing Eq. (36) to Eq. (32), it should be noted that they do not yield identical constitutive relations for the stress, even when $\lambda_a = \widetilde{\lambda}_a$ and $\Psi_a = \widetilde{\Psi}_a$. This result emphasizes that, even in the limiting case of instantaneous biphasic response where it is acceptable to use the above uncoupled formulation, the stress-strain re-

sponse is not identical to the more general coupled formulation.

It is interesting to note that this limitation can be overcome if the coupled and uncoupled constitutive formulations are selected such that the deviatoric part of the stress tensor $\mathbf{T}^e$ has the same form when $J=1$ (see Appendix). In that case, the two formulations will only differ by a hydrostatic stress term and they will produce identical displacement and strain fields, and identical total stress $\mathbf{T}$ in the instantaneous biphasic (or incompressible elastic) response; but the pressure p and the stress $\mathbf{T}^e$ will not be the same. From a practical perspective, if one uses a finite element implementation of incompressible elasticity which employs an uncoupled strain energy formulation, but would like to simulate the instantaneous response of a biphasic material whose strain energy is coupled, the analysis can proceed as follows: (a) Determine the deviatoric stress from the coupled biphasic constitutive relation; (b) derive an uncoupled formulation which yields an identical deviatoric stress when $J=1$, and implement it into the finite element analysis (for example, see Eqs. (18) and (28)); (c) substitute the strain tensor obtained from the finite element analysis into the coupled constitutive relation to get the stress $\mathbf{T}^e$; (d) use this $\mathbf{T}^e$ and the total stress $\mathbf{T}$ obtained from the finite element analysis to evaluate the pressure for the coupled formulation, $p = \mathrm{tr}(\mathbf{T}^e - \mathbf{T})/3$.

Biphasic Finite Element Formulation. To illustrate the equivalence of the instantaneous biphasic and incompressible elastic response under finite deformation, a custom-written biphasic finite element code was developed based on a $\mathbf{u}$-p formulation [32]. The weak form of the weighted residual formulation for this problem, based on substituting Eq. (1) into Eq. (2), and on Eq. (4), is given by

$$I^m = \int_V (\mathbf{w} \cdot \mathrm{grad}\, \xi - \xi\, \mathrm{div}\, \mathbf{v})dV - \int_S \xi w_n dS = 0 \qquad (38)$$

$$I^t = \int_V \mathbf{T}{:}\mathrm{grad}\, \boldsymbol{\xi} dV - \int_S \boldsymbol{\xi} \cdot \mathbf{t}\, dS = 0 \qquad (39)$$

where $\mathbf{t}=\mathbf{Tn}$ is the traction on the solid matrix, ξ is a scalar weight function, $\boldsymbol{\xi}=\xi\mathbf{e}_j$ is a vector weight function and $\mathbf{e}_j$ are the unit vectors of an orthonormal basis. V and S represent the volume and surface of the material region in the current configuration. Note that the weight function ξ (which is also the shape function) is selected to be the same for both equations. In general, $\mathbf{T}$ and $\mathbf{w}$ are functions of $\mathbf{C}$ and p. For a nonlinear analysis requiring an iterative solution scheme we use a Taylor series expansion of these functions to first order terms,

$$I + \delta I \approx 0 \qquad (40)$$

where I represents either I^m or I^t. To evaluate δI it is convenient to pull back the above integrals to the reference configuration, perform the functional differentiation, then push them forward to the current configuration [23]. This is achieved by making use of the standard relations between spatial and material representations of these equations, including the relation between the Cauchy stress and 2nd Piola-Kirchhoff stress, $\mathbf{T}=J^{-1}\mathbf{FSF}^T$, and the basic relations $\mathrm{grad}\, \xi = \mathbf{F}^{-T}\, \mathrm{Grad}\, \xi$, $\mathrm{grad}\, \boldsymbol{\xi} = (\mathrm{Grad}\, \boldsymbol{\xi})\mathbf{F}^{-1}$, $\mathrm{grad}\, \mathbf{v} = (\mathrm{Grad}\, \mathbf{v})\mathbf{F}^{-1}$ and $dV = J\, dV_0$, where V_0 represents the volume in the reference configuration. Using these relations, the volume integrals in Eqs. (38) and (39) become

$$\int_V (\mathbf{w} \cdot \mathrm{grad}\, \xi - \xi\, \mathrm{div}\, \mathbf{v})dV$$

$$= \int_{V_0} (\mathbf{w} \cdot \mathbf{F}^{-T}\mathrm{Grad}\, \xi - \xi\, \mathrm{tr}[(\mathrm{Grad}\, \mathbf{v})\mathbf{F}^{-1}])J\, dV_0 \qquad (41)$$

$$\int_V \mathbf{T}{:}\mathrm{grad}\, \boldsymbol{\xi}\, dV = \int_{V_0} \mathbf{FS}{:}\, \mathrm{Grad}\, \boldsymbol{\xi}\, dV_0 \qquad (42)$$

Differentiating the integrals over V_0, making use of the standard relations

$$\delta \mathbf{C} = 2\mathbf{F}^T\, \mathrm{grad}^S(\delta\mathbf{u})\mathbf{F}, \quad \delta J = J\, \mathrm{div}\, \delta\mathbf{u} \qquad (43)$$

$$\mathrm{grad}^S(\delta\mathbf{u}) = (\mathrm{grad}\, \delta\mathbf{u} + \mathrm{grad}^T\, \delta\mathbf{u})/2 \qquad (44)$$

$$\delta\mathbf{F}^{-1} = -\mathbf{F}^{-1}\, \mathrm{grad}\, \delta\mathbf{u} \qquad (45)$$

where $\mathrm{grad}^S[\cdot]$ is the symmetric gradient operator and $\delta\mathbf{u}$ is the incremental displacement, then reverting back to the current configuration, it is found that

$$\delta\left(\int_V [\mathbf{w} \cdot \mathrm{grad}\, \xi - \xi\, \mathrm{div}\, \mathbf{v}]dV \right)$$

$$= \int_V (\delta\mathbf{w} \cdot \mathrm{grad}\xi + \mathbf{w} \cdot [(\mathrm{div}\, \delta\mathbf{u})\mathbf{I} - \mathrm{grad}^T\, \delta\mathbf{u}]\mathrm{grad}\, \xi)dV$$

$$- \int_V \xi[\mathrm{div}\, \delta\mathbf{v} + (\mathrm{div}\, \mathbf{v})(\mathrm{div}\, \delta\mathbf{u}) - \mathrm{grad}\, \mathbf{v}{:}\mathrm{grad}^T\, \delta\mathbf{u}]dV$$

$$(46)$$

$$\delta\left(\int_V \mathbf{T}{:}\mathrm{grad}\, \boldsymbol{\xi}\, dV \right) = \int_V [\mathrm{grad}\, \boldsymbol{\xi}{:}\delta\mathbf{T} + (\mathrm{grad}^T\, \delta\mathbf{u})(\mathrm{grad}\, \boldsymbol{\xi}){:}\mathbf{T}]dV$$

$$(47)$$

We now adopt the constitutive assumption of Eq. (12) which yields $\mathbf{w}=-\mathbf{K}\, \mathrm{grad}\, p$. We further assume that the permeability tensor is only a function of the relative volume change J and that this dependence is the same for all components of $\mathbf{K}$. These assumptions imply that $\mathbf{K}=k(J)\mathbf{I}$ where $k(J)$ may be given by Eq. (13). Given these constitutive restrictions it follows that

$$\delta\mathbf{w} = \frac{Jk'(J)}{k(J)}(\mathrm{div}\, \delta\mathbf{u})\mathbf{w} - k(J)\mathrm{grad}\, \delta p \qquad (48)$$

In principle it is now possible to substitute Eq. (48) into Eq. (46) and the resulting expression, along with Eq. (38), into Eq. (40) to obtain the form needed in the finite element implementation. However this form yields a non-symmetric stiffness matrix, which is computationally disadvantageous. A way around this problem is to neglect the terms in Eqs. (46) and (48) that depend on $\delta\mathbf{u}$ so that the nonlinear equation is given instead by

$$\int_V [-\mathrm{grad}\, \xi \cdot \mathbf{K}\, \mathrm{grad}\, \delta p - \xi\, \mathrm{div}\, \delta\mathbf{v}]dV$$

$$\approx \int_S \xi w_n dS - \int_V (\mathbf{w} \cdot \mathrm{grad}\, \xi - \xi\, \mathrm{div}\, \mathbf{v})dV \qquad (49)$$

It was found that neglecting these terms to yield a symmetric global stiffness matrix did not compromise convergence of the nonlinear iterative solution scheme. Substituting Eq. (47) into Eq. (40) and using Eq. (39) yields

$$\int_V [-\delta p\, \mathrm{div}\, \boldsymbol{\xi} + \mathrm{grad}\, \boldsymbol{\xi}{:}\overset{4}{\mathbf{C}}{:}\delta\boldsymbol{\varepsilon} + (\mathrm{grad}^T\, \delta\mathbf{u})(\mathrm{grad}\, \boldsymbol{\xi}){:}\mathbf{T}]dV$$

$$\approx \int_S \boldsymbol{\xi} \cdot \mathbf{t}\, dS - \int_V \mathbf{T}{:}\mathrm{grad}\boldsymbol{\xi} + dV \qquad (50)$$

where we have used $\delta\mathbf{T}=-\delta p\mathbf{I}+\delta\mathbf{T}^e$, and $\delta\mathbf{T}^e=\overset{4}{\mathbf{C}}{:}\mathrm{grad}^S(\delta\mathbf{u})$. Since the incremental solid matrix velocity is given by $\delta\mathbf{v}$

$=\delta\mathbf{u}/\delta t$, the two relations above produce a linear set of equations in the unknowns $\delta\mathbf{u}$ and δp upon discretization. In the iterative application of these equations, p, $\mathbf{v}$, $\mathbf{C}$, $\mathbf{w}$, and $\mathbf{T}$ represent values from the previous iteration, which are then updated using $\mathbf{u}\leftarrow\mathbf{u}+\delta\mathbf{u}$ and $p\leftarrow p+\delta p$.

For the current study, an axisymmetric finite element formulation was used, with 8-node isoparametric (serendipity) quadrilateral elements. It was found that an incompressible response could be enforced numerically at the first time step $t=\delta t$ (equivalent to $t=0^+$) when substituting $(1/J)(DJ/Dt)$ for div $\mathbf{v}$ on the right-hand side of Eq. (49).

Early-Time Biphasic Response. Having established the equivalence between the instantaneous biphasic and incompressible elastic formulations, it is necessary to estimate how small the initial time increment of a numerical biphasic analysis should be, to yield a nearly-incompressible response. Substituting Eq. (1) into Eq. (2) yields $-\mathrm{grad}\,p + \mathrm{div}\,\mathbf{T}^e = \mathbf{0}$, into which we can substitute the relation $\mathbf{w} = -\mathbf{K}\,\mathrm{grad}\,p$ to produce $\mathbf{w}+\mathbf{K}\,\mathrm{div}\,\mathbf{T}^e = \mathbf{0}$. Taking the divergence of this expression and using Eq. (4) yields

$$\mathrm{div}\,\mathbf{v} = \mathrm{div}(\mathbf{K}\,\mathrm{div}\,\mathbf{T}^e) \tag{51}$$

At the initial time increment δt, the velocity and stress are given by $\mathbf{v} \approx \delta\mathbf{u}/\delta t$ and $\mathbf{T}^e \approx \overset{4}{\mathbf{C}}:\delta\boldsymbol{\varepsilon}$, where $\delta\boldsymbol{\varepsilon}$ is given by Eq. (43). Substituting these expressions into the above equation, we find that a sufficient condition to produce a vanishing div $\mathbf{v}$ is to have

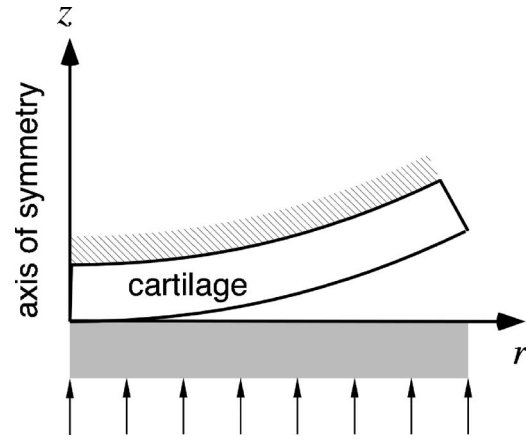$$\frac{\delta t\|\overset{4}{\mathbf{C}}\|\,\|\mathbf{K}\|}{\Delta^2} \to 0 \tag{52}$$

where Δ is a characteristic length for the given problem. Thus $\Delta^2/\delta t\|\overset{4}{\mathbf{C}}\|\,\|\mathbf{K}\|$ effectively acts as a penalty number for enforcing incompressibility, and this nondimensional number should be selected as large as practicable to achieve an isochoric response; this is equivalent to picking

$$\delta t \ll \Delta^2/\|\overset{4}{\mathbf{C}}\|\,\|\mathbf{K}\| \tag{53}$$

Unconfined Compression. An unconfined compression 2D axisymmetric finite element analysis was performed for a biphasic disk of radius 3 mm and thickness 0.5 mm, loaded with rigid impermeable frictionless platens. The lateral surface of the disk is exposed to atmospheric conditions, so that the fluid pressure p on this surface is prescribed to be zero. In this analysis, the strain energy density of Eq. (31) was used, where W_0 is given by Eq. (17) and Ψ_a by Eq. (34). The material coefficients were $\lambda = 0$ MPa, $\mu = 4$ MPa, $k_0 = 2.7\times10^{-3}$ mm^4/N s, $\varphi_0^w = 0.8$, $\alpha = 2$, $M = 2.2$, $\xi_a = 1000$ MPa, and $\beta_a = 3.6$ $(a=1-3)$. The biphasic response was evaluated at $\delta t = 0.001$ s. The mesh consisted of 40 elements along the radial direction and one element through the depth; biases were created to refine the mesh near the radial edge. The biphasic response was compared to the incompressible elastic response for a disk (or equivalently, a cylindrical bar), which can be derived in closed-form for this problem,

$$\begin{aligned} \bar{p} &= \mu\left(\frac{1}{\lambda_z}-1\right) \\ \bar{T}_{zz} &= \mu\left(\lambda_z^2 - \frac{1}{\lambda_z}\right) + \beta_z\xi_z\lambda_z(\lambda_z-1)^{\beta_z-1} \end{aligned} \quad \lambda_z > 1 \tag{54}$$


Fig. 1 Schematic of the axisymmetric finite element contact analysis

$$\begin{aligned} \bar{p} &= \mu\left(\frac{1}{\lambda_z}-1\right) + \frac{1}{\sqrt{\lambda_z}}\beta_r\xi_r\left(\frac{1}{\sqrt{\lambda_z}}-1\right)^{\beta_r-1} \\ \bar{T}_{zz} &= \mu\left(\lambda_z^2 - \frac{1}{\lambda_z}\right) - \beta_r\xi_r\frac{1}{\sqrt{\lambda_z}}\left(\frac{1}{\sqrt{\lambda_z}}-1\right)^{\beta_r-1} \end{aligned} \quad \lambda_z < 1 \tag{55}$$

Here, λ_z represents the axial stretch; the first pair of solutions corresponds to tensile loading of a bar while the second pair represents unconfined compression of a disk. In the biphasic finite element analysis, a displacement of -0.1 mm was prescribed on the top loading platen while the bottom loading platen was kept stationary; these boundary conditions produce a uniform axial stretch of $\lambda_z = 0.8$.

Contact Analyses. A 2D axisymmetric finite element frictionless contact analysis was performed between a spherical biphasic layer anchored to a rigid impermeable substrate and a flat impermeable rigid surface (Fig. 1). This geometry was representative of the articular layer of an immature bovine humeral head, with a cartilage surface radius of 46.3 mm and a cartilage layer thickness of 0.8 mm. The deformation at the center of the articular layer was set to 0.095 mm ($\sim$12% of the thickness). In the first analysis, the uncoupled isotropic strain energy density of Eq. (27) was used, with material coefficients $\lambda = 0$ MPa, $\mu = 4$ MPa, $k_0 = 2.7\times10^{-3}$ mm^4/N s, $\varphi_0^w = 0.8$, $\alpha = 2$, and $M = 2.2$. In the second analysis, this strain energy density was supplemented with the tension-only contribution as shown in Eq. (35), where the form of $\tilde{\Psi}_a(\tilde{\lambda}_a)$ was the same as that of $\Psi_a(\lambda_a)$ in Eq. (34), with $\xi_a = 1000$ MPa and $\beta_a = 3.6$ $(a=1-3)$. In both analyses, the biphasic response was evaluated at $\delta t = 0.001$ s. The mesh consisted of 20 elements through the thickness and 50 elements along the radial direction, for a total of 1000 elements; biases were created to refine the mesh near the articular surface, the rigid bony substrate, and the edge of the contact region (Fig. 2).

The results of the biphasic contact analyses were compared to those of equivalent contact problems with an incompressible elastic model, using NIKE3D [33]. The articular geometry was modeled using a 3D mesh with identical dimensions as for the biphasic analysis; due to symmetry, only a quarter of the spherical layer was modeled, with 20 isoparametric 8-node brick elements through the thickness, 50 along the radial direction, and 14 along the circumferential direction. The element formulation was based on a three-field variational principle that allows the modeling of nearly-incompressible materials without element locking [25]. Fully incompressible material response was enforced via an augmented Lagrangian method. The NIKE3D code was customized to
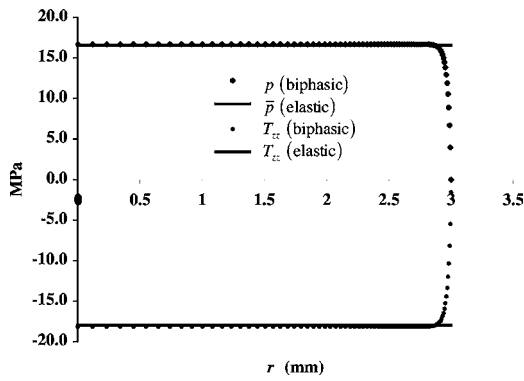
Fig. 2 Results of unconfined compression analysis of a cylindrical disk. For this axisymmetric analysis, the mesh extends from $r=0$ to $r=3$ mm. Symbols represent the biphasic response at $\delta t=0.001$ s and solid lines represent the analytical solution for the incompressible elastic response of Eq. (54), evaluated at $\lambda_z=0.8$.

incorporate the desired constitutive relations, including tension-compression nonlinearity. The material properties μ, ξ_a, and β_a were the same as for the biphasic layer.

Results

The results of the unconfined compression analysis are presented in Fig. 2, showing the pressure and axial normal stress for the biphasic analysis, p and T_{zz}, as well as the corresponding incompressible elastic pressure $\bar{p}$ and axial normal stress $\bar{T}_{zz}$. The short-term biphasic response is identically equal to the incompressible elastic response given by the analytical solution of Eq. (54), except in a very narrow boundary layer at the radial edge of the disk.
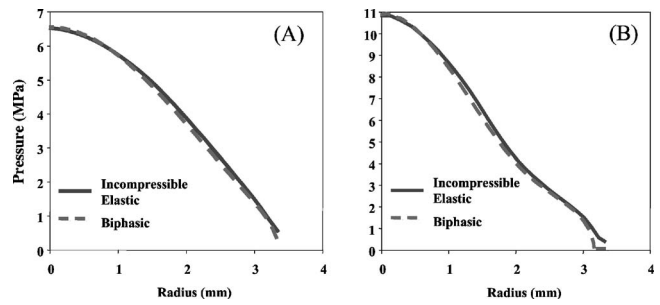
For the contact analyses, comparisons of the normal component of the traction, $t_n^*=\mathbf{n}\cdot\mathbf{Tn}$, and biphasic and incompressible elastic pressures p and $\bar{p}$, are presented in Figs. 3 and 4 for both analyses, showing nearly identical results inside the contact region. Note that $\bar{p}$ does not reduce exactly to zero right outside the contact region, whereas p does; this difference can be attributed to the fact that no boundary conditions can be imposed on $\bar{p}$, whereas p is explicitly set to zero outside of the contact region. Contour plots of the pressures and radial and axial normal Lagrangian strains, E_{rr} and E_{zz}, are also shown for the biphasic and incompressible elastic cases of the second analysis, in Figs. 5–7. Both cases show nearly identical results.

Discussion

This study demonstrates from basic principles that the instantaneous response of a biphasic material is equivalent to the response of an incompressible elastic material for arbitrary deformations
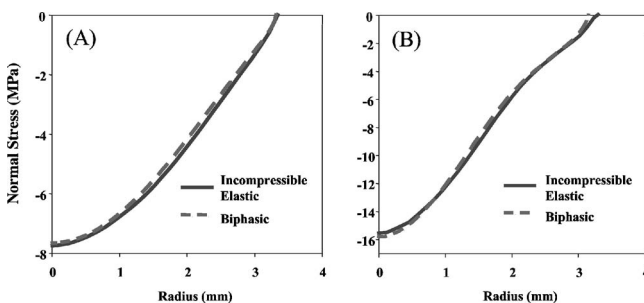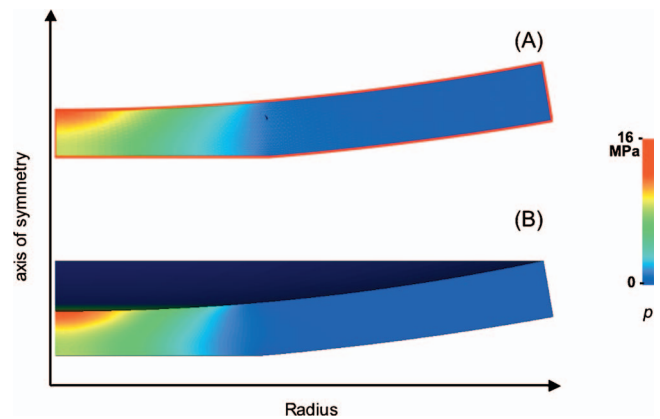

Fig. 3 Normal traction at the contact interface for the first and second analyses (the latter with tension-compression nonlinearity), for biphasic and incompressible elastic cases

and material symmetry, and provides practical guidelines for the validity of this equivalence over the short-term biphasic response. This result generalizes the special cases demonstrated in earlier studies [1,4,6–9]. The stress and solid displacement are identical and the interstitial fluid pressure in a biphasic analysis is equal to the hydrostatic pressure in an incompressible elastic analysis everywhere except at permeable boundaries, where the pressure in the biphasic analysis reduces to the prescribed boundary condition (ambient pressure) over an infinitesimally thin boundary layer.

This general result was illustrated with an unconfined compression analysis of a biphasic disk, and with two sample finite deformation contact analyses, using a custom-written biphasic finite element program and the well-validated NIKE3D program, customized to incorporate the desired constitutive relations. The un-

Fig. 4 Fluid pressure at the contact interface for the first and second analyses, for biphasic and incompressible elastic cases

Fig. 5 Contour plot of the fluid pressure for (a) the biphasic case and (b) the incompressible elastic case, for the second analysis
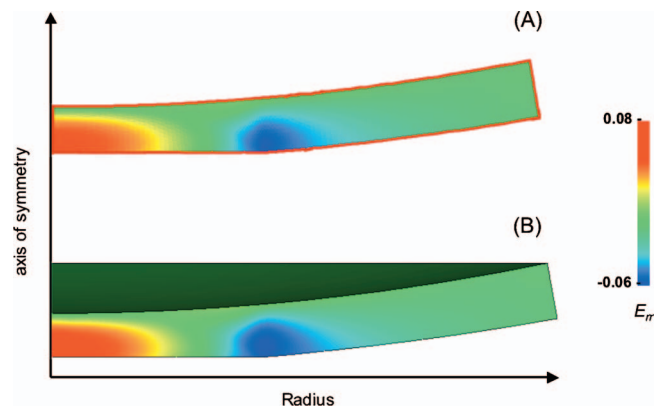
Fig. 6 Radial normal Lagrangian strain E_{rr} for (a) the biphasic case and (b) the incompressible elastic case, for the second analysis
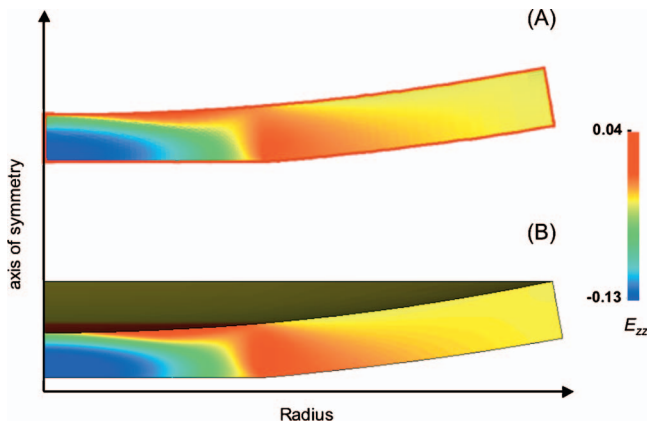
Fig. 7 Axial normal Lagrangian strain E_{zz} for (a) the biphasic case and (b) the incompressible elastic case, for the second analysis

confined compression analysis neatly illustrates how the fluid pressure $\bar{p}$ in the incompressible elastic analysis is equal to the pressure p in the biphasic analysis everywhere along r, except in a thin boundary layer near the permeable radial edge (Fig. 2). From theory, we know that the boundary layer in a biphasic analysis is infinitely thin at $t=0^+$; however, in a numerical implementation such as the one shown here, the biphasic solution is evaluated at a small, but finite time step. Thus, the boundary layer thickness is related to the size of this initial time increment. This example clarifies that if one conducts an incompressible elastic analysis to simulate the instantaneous biphasic response, one should expect $\bar{p}$ to be an accurate representation of p everywhere except at a permeable boundary, where one should (mentally) substitute the solution for $\bar{p}$ with the appropriate boundary condition for p.

The agreement observed in the contact analyses between the two approaches is remarkable, especially considering that the biphasic analysis is based on a 2D axisymmetric implementation in cylindrical coordinates while the NIKE3D analysis is three-dimensional and in Cartesian coordinates. From the contour plots of the pressure (Fig. 5), it is evident that the biphasic and elastic analyses yielded nearly identical results everywhere inside the articular layer. The permeable boundaries in the biphasic analysis are the articular surface outside of the contact region, and the lateral edge. Based on the prescribed boundary conditions, the fluid pressure p was set to zero at these locations. In contrast, no boundary condition could be imposed on $\bar{p}$. Nevertheless, $\bar{p}$ nearly reduced to zero at these boundaries, in close agreement with p (Fig. 4). This suggests that, for this type of contact analyses, the instantaneous biphasic and incompressible elastic predictions do not differ appreciably even at permeable boundaries. However, it is important not to generalize this special case to all types of problems, as shown for example in the analysis of unconfined compression in Fig. 1.

The results of this study provide a rationale for using available finite element codes for incompressible elastic materials as a practical substitute for biphasic analyses, as long as only the short-time biphasic response is sought. In the application of these analyses to the study of biological tissues, the physiological relevance of the short-time response depends on the problem being examined. As shown in Eq. (52), the characterization of the "short-time" response depends on the modulus, permeability, and characteristic dimensions of the tissue. For example, for the above articular cartilage contact problem, $\|\overset{4}{\mathbf{C}}\| \sim 650$ MPa (based on the finite element results), $\|\mathbf{K}\| \sim 2.7 \times 10^{-3}$ mm^4/N s, and $\Delta \sim 3$ mm (the radius of the contact area [34]), so that the short-time response, calculated from these values using Eq. (53), corresponds

to $\delta t \ll 5$ s. In other words, the elastic incompressible contact analysis would be representative of biphasic contact analyses where loading occurs over a time span of ~ 0.5 s or less.

The equivalence between the instantaneous biphasic and incompressible elastic responses is valid for any constitutive model, as long as the biphasic constitutive equations reduce to the incompressible elastic equations when $J=1$, as shown for example in Eq. (11). However, depending on the finite element implementation for incompressible elasticity, some limitations may be imposed on the choice of constitutive formulations, as shown in the case of uncoupled strain energy densities. These limitations do not invalidate the general equivalence, but may impose some practical restrictions that should be heeded in any specific application. Indeed, several popular finite element programs, including ABAQUS (ABAQUS, Inc., Providence, RI) and FEAP (University of California, Berkeley), use an uncoupled strain energy implementation for modeling incompressible elastic solids. These restrictions can be overcome as outlined in the methods above, by properly postprocessing the results of the incompressible elastic finite element analysis to reproduce the instantaneous biphasic values of p and $\mathbf{T}^e$ for any desired coupled constitutive relation.

The finite element formulation for the biphasic finite deformation analysis (Eqs. (49) and (50)) is based on a spatial description [23] and differs in its details from the formulations adopted by others [35–39]. It is also presented in a form which accommodates non-Cartesian orthonormal coordinate bases, such as cylindrical and spherical coordinates [40], whereas most formulations are expressed for Cartesian bases, whether explicitly stated or not [23]. In practice, the details of the biphasic finite element implementation may influence the short-time response. As noted above, our implementation yielded an isochoric short-time response only when the discretized form of div $\mathbf{v}$ was replaced with a discretized form of $(1/J)(DJ/Dt)$ on the right-hand side of Eq. (49).

In summary, this study presents a practical alternative for analyzing the short-term response of a biphasic solid-fluid mixture using incompressible elasticity by demonstrating a general equivalence between these two theories under arbitrary deformations. The only difference between the theories occurs in an infinitely thin layer at boundaries where the fluid pressure needs to be prescribed in a biphasic analysis. This theoretical equivalence was demonstrated using finite element analyses of a contact problem representative of articular joints, showing the expected agreement. While the mathematical equivalence is universal, caution must be exercised when selecting constitutive relations which remain physically meaningful if the finite element implementation of the incompressible elastic response employs an uncoupled strain energy formulation.

Acknowledgment

Appendix

Tensor Products. The double contraction operator is used in a variety of combinations between tensors of various orders [23]. For second-order tensors $\mathbf{S}$ and $\mathbf{T}$, the contraction is simply $\mathbf{S}:\mathbf{T} = S_{ij}T_{ij}$. For a fourth-order tensor $\overset{4}{\mathbf{M}}$, third-order tensor $\overset{3}{\mathbf{N}}$, and second-order tensor $\mathbf{T}$, we have $(\overset{4}{\mathbf{M}}:\mathbf{T})_{ij}=M_{ijkl}T_{kl}$, $(\mathbf{T}:\overset{4}{\mathbf{M}})_{ij} = T_{kl}M_{klij}$, $(\overset{3}{\mathbf{N}}:\mathbf{T})_i=N_{ijk}T_{jk}$, $(\overset{3}{\mathbf{N}}:\overset{4}{\mathbf{M}})_{ijk}=N_{ilm}M_{lmjk}$, etc. The double contraction of two fourth-order tensors $\overset{4}{\mathbf{M}}$ and $\overset{4}{\mathbf{N}}$ yields a fourth-

order tensor, $(\mathbf{M}:\mathbf{N})_{ijkl} = M_{ijmn}N_{mnkl}$.

The tensor dyadic products $\underline{\overline{\otimes}}$ and $\otimes$ are defined by [26]

$$(\mathbf{S} \otimes \mathbf{T})_{ijkl} = S_{ij}T_{kl} \tag{A1}$$

$$(\mathbf{S}\underline{\otimes}\mathbf{T})_{ijkl} = S_{ik}T_{jl} \tag{A2}$$

$$(\mathbf{S}\underline{\overline{\otimes}}\mathbf{T})_{ijkl} = \frac{1}{2}(S_{ik}T_{jl} + S_{il}T_{jk}) \tag{A3}$$

Coupled and Uncoupled Formulations. Using Eqs. (15) and (32), the deviatoric part of the stress tensor $\mathbf{T}^e$ in a general (coupled) constitutive relation is

$$\operatorname{dev} \mathbf{T}^e = \operatorname{dev}\left(2J^{-1}\mathbf{F}\frac{\partial W}{\partial \mathbf{C}}\mathbf{F}^T + J^{-1}\sum_{a=1}^{3} \lambda_a \frac{\partial \Psi_a}{\partial \lambda_a}\left(\mathbf{A}_a - \frac{1}{3}\mathbf{I}\right) \right) \tag{A4}$$

Similarly, using Eqs. (22), (24), and (36), the deviatoric part of $\mathbf{T}^e$ in an uncoupled constitutive relation is given by

$$\operatorname{dev} \mathbf{T}^e = \operatorname{dev}\left(2J^{-1}\widetilde{\mathbf{F}}\frac{\partial \widetilde{W}}{\partial \widetilde{\mathbf{C}}}\widetilde{\mathbf{F}}^T + J^{-1}\sum_{a=1}^{3} \widetilde{\lambda}_a \frac{\partial \widetilde{\Psi}_a}{\partial \widetilde{\lambda}_a}\left(\mathbf{A}_a - \frac{1}{3}\mathbf{I}\right) \right) \tag{A5}$$

When $J = 1$, it follows that $\widetilde{\mathbf{F}} = \mathbf{F}$, $\widetilde{\mathbf{C}} = \mathbf{C}$, and $\widetilde{\lambda}_a = \lambda_a$. Thus, if $W(\mathbf{C})$ and $\widetilde{W}(\widetilde{\mathbf{C}})$ are selected to have the same form, as are $\Psi_a(\lambda_a)$ and $\widetilde{\Psi}_a(\widetilde{\lambda}_a)$, the coupled and uncoupled formulations will yield identical deviatoric stresses under isochoric deformations.

References

[1] Mow, V. C., Kuei, S. C., Lai, W. M., and Armstrong, C. G., 1980, "Biphasic Creep and Stress Relaxation of Articular Cartilage in Compression: Theory and Experiments," ASME J. Biomech. Eng., **102**, pp. 73–84.

[2] Cohen, B., Lai, W. M., and Mow, V. C., 1998, "A Transversely Isotropic Biphasic Model for Unconfined Compression of Growth Plate and Chondroepiphysis," ASME J. Biomech. Eng., **120**, pp. 491–496.

[3] Soulhat, J., Buschmann, M. D., and Shirazi-Adl, A., 1999, "A Fibril-Network-Reinforced Biphasic Model of Cartilage in Unconfined Compression," ASME J. Biomech. Eng., **121**, pp. 340–347.

[4] Soltz, M. A., and Ateshian, G. A., 2000, "A Conewise Linear Elasticity Mixture Model for the Analysis of Tension-Compression Nonlinearity in Articular Cartilage," ASME J. Biomech. Eng., **122**, pp. 576–586.

[5] Bachrach, N. M., Mow, V. C., and Guilak, F., 1998, "Incompressibility of the Solid Matrix of Articular Cartilage Under High Hydrostatic Pressures," J. Biomech., **31**, pp. 445–451.

[6] Armstrong, C. G., Lai, W. M., and Mow, V. C., 1984, "An Analysis of the Unconfined Compression of Articular Cartilage," ASME J. Biomech. Eng., **106**, pp. 165–173.

[7] Brown, T. D., and Singerman, R. J., 1986, "Experimental Determination of the Linear Biphasic Constitutive Coefficients of Human Fetal Proximal Femoral Chondroepiphysis," J. Biomech., **19**, pp. 597–605.

[8] Mak, A. F., Lai, W. M., and Mow, V. C., 1987, "Biphasic Indentation of Articular Cartilage. I. Theoretical Analysis," J. Biomech., **20**, pp. 703–714.

[9] Ateshian, G. A., Lai, W. M., Zhu, W. B., and Mow, V. C., 1994, "An Asymptotic Solution for the Contact of Two Biphasic Cartilage Layers," J. Biomech., **27**, pp. 1347–1360.

[10] Armstrong, C. G., and Mow, V. C., 1982, "Variations in the Intrinsic Mechanical Properties of Human Articular Cartilage With Age, Degeneration, and Water Content," J. Bone Jt. Surg., Am. Vol., **64**, pp. 88–94.

[11] Chahine, N. O., Wang, C. C., Hung, C. T., and Ateshian, G. A., 2004, "Anisotropic Strain-Dependent Material Properties of Bovine Articular Cartilage in the Transitional Range From Tension to Compression," J. Biomech., **37**, pp. 1251–1261.

[12] Huang, C. Y., Stankiewicz, A., Ateshian, G. A., and Mow, V. C., 2005, "Anisotropy, Inhomogeneity, and Tension-Compression Nonlinearity of Human

[13] Kempson, G. E., Freeman, M. A., and Swanson, S. A., 1968, "Tensile Properties of Articular Cartilage," Nature (London), **220**, pp. 1127–1128.

[14] Hayes, W. C., Keer, L. M., Herrmann, G., and Mockros, L. F., 1972, "A Mathematical Analysis for Indentation Tests of Articular Cartilage," J. Biomech., **5**, pp. 541–551.

[15] Eberhardt, A. W., Keer, L. M., Lewis, J. L., and Vithoontien, V., 1990, "An Analytical Model of Joint Contact," ASME J. Biomech. Eng., **112**, pp. 407–413.

[16] Carter, D. R., and Beaupre, G. S., 1999, "Linear Elastic and Poroelastic Models of Cartilage Can Produce Comparable Stress Results: A Comment on Tanck Et Al. (J Biomech 32:153–161, 1999)," J. Biomech., **32**, pp. 1255–1257.

[17] Wong, M., and Carter, D. R., 1990, "Theoretical Stress Analysis of Organ Culture Osteogenesis," Bone (N.Y.), **11**, pp. 127–131.

[18] Bowen, R. M., 1980, "Incompressible Porous Media Models by Use of the Theory of Mixtures," Int. J. Eng. Sci., **18**, pp. 1129–1148.

[19] Huyghe, J. M., and Janssen, J. D., 1997, "Quadriphasic Mechanics of Swelling Incompressible Porous Media," Int. J. Eng. Sci., **35**, pp. 793–802.

[20] Holmes, M. H., and Mow, V. C., 1990, "The Nonlinear Characteristics of Soft Gels and Hydrated Connective Tissues in Ultrafiltration," J. Biomech., **23**, pp. 1145–1156.

[21] Lai, W. M., and Mow, V. C., 1980, "Drag-Induced Compression of Articular Cartilage During a Permeation Experiment," Biorheology, **17**, pp. 111–123.

[22] Gu, W. Y., Yao, H., Huang, C. Y., and Cheung, H. S., 2003, "New Insight Into Deformation-Dependent Hydraulic Permeability of Gels and Cartilage, and Dynamic Behavior of Agarose Gels in Confined Compression," J. Biomech., **36**, pp. 593–598.

[23] Bonet, J., and Wood, R. D., 1997, *Nonlinear Continuum Mechanics for Finite Element Analysis*, Cambridge University Press, Cambridge.

[24] Simo, J. C., Taylor, R. L., and Pister, K. S., 1985, "Variational and Projection Methods for the Volume Constraint in Finite Deformation Elastoplasticity," Comput. Methods Appl. Mech. Eng., **51**, pp. 177–208.

[25] Weiss, J. A., Maker, B. N., and Govindjee, S., 1996, "Finite Element Implementation of Incompressible, Transversely Isotropic Hyperelasticity," Comput. Methods Appl. Mech. Eng., **135**, pp. 107–128.

[26] Curnier, A., He, Q. C., and Zysset, P., 1995, "Conewise Linear Elastic Materials," J. Elast., **37**, pp. 1–38.

[27] Quapp, K. M., and Weiss, J. A., 1998, "Material Characterization of Human Medial Collateral Ligament," ASME J. Biomech. Eng., **120**, pp. 757–763.

[28] Baer, A. E., Laursen, T. A., Guilak, F., and Setton, L. A., 2003, "The Micromechanical Environment of Intervertebral Disc Cells Determined by a Finite Deformation, Anisotropic, and Biphasic Finite Element Model," ASME J. Biomech. Eng., **125**, pp. 1–11.

[29] Lanir, Y., 1983, "Constitutive Equations for Fibrous Connective Tissues," J. Biomech., **16**, pp. 1–12.

[30] Lanir, Y., 1987, "Biorheology and Fluid Flux in Swelling Tissues, Ii. Analysis of Unconfined Compressive Response of Transversely Isotropic Cartilage Disc," Biorheology, **24**, pp. 189–205.

[31] Laasanen, M. S., Toyras, J., Korhonen, R. K., Rieppo, J., Saarakkala, S., Nieminen, M. T., Hirvonen, J., and Jurvelin, J. S., 2003, "Biomechanical Properties of Knee Articular Cartilage," Biorheology, **40**, pp. 133–140.

[32] Wayne, J. S., Woo, S. L., and Kwan, M. K., 1991, "Application of the U-P Finite Element Method to the Study of Articular Cartilage," ASME J. Biomech. Eng., **113**, pp. 397–403.

[33] Maker, B. N., Ferencz, R. M., and Hallquist, J. O., 1990, "Nike3D: A Nonlinear, Implicit, Three-Dimensional Finite Element Code for Solid and Structural Mechanics," LLNL Technical Report No. UCRL-MA 105268.

[34] Kelkar, R., and Ateshian, G. A., 1999, "Contact Creep of Biphasic Cartilage Layers," ASME J. Appl. Mech., **66**, pp. 137–145.

[35] Almeida, E. S., and Spilker, R. L., 1997, "Mixed and Penalty Finite Element Models for the Nonlinear Behavior of Biphasic Soft Tissues in Finite Deformation: Part I—Alternate Formulations," Comput. Methods Biomech. Biomed. Eng., **1**, pp. 25–46.

[36] Levenston, M. E., Frank, E. H., and Grodzinsky, A. J., 1998, "Variationally Derived 3-Field Finite Element Formulations for Quasistatic Poroelastic Analysis of Hydrated Biological Tissues," Comput. Methods Appl. Mech. Eng., **156**, pp. 231–246.

[37] Suh, J. K., and Spilker, R. L., 1991, "Penalty Finite Element Analysis for Non-Linear Mechanics of Biphasic Hydrated Soft Tissue Under Large Deformation," Int. J. Numer. Methods Eng., **32**, pp. 1411–1439.

[38] Diebels, S., and Ehlers, W., 1996, "Dynamic Analysis of a Fully Saturated Porous Medium Accounting for Geometrical and Material Non-Linearities," Int. J. Numer. Methods Eng., **39**, pp. 81–97.

[39] Simon, B. R., Kaufmann, M. V., McAfee, M. A., and Baldwin, A. L., 1993, "Finite Element Models for Arterial Wall Mechanics," ASME J. Biomech. Eng., **115**, pp. 489–496.

[40] Meng, X. N., LeRoux, M. A., Laursen, T. A., and Setton, L. A., 2002, "A Nonlinear Finite Element Formulation for Axisymmetric Torsion of Biphasic Materials," Int. J. Solids Struct., **39**, pp. 879–895.

[12] (cont.) Glenohumeral Cartilage in Finite Deformation," J. Biomech., **38**, pp. 799–809.